Diagnostic and Interventional Imaging (2018) xxx, xxx—xxx

SOLICITED REVIEW / *Genitourinary imaging*

Characterization of small (<4 cm) solid renal masses by computed tomography and magnetic resonance imaging: Current evidence and further development

N. Schieda [a], R.S. Lim [a], M.D.F. McInnes [a], I. Thomassin [b], R. Renard-Penna [b], S. Tavolaro [b], F.H. Cornelis [b,*]

[a] *Department of Medical Imaging, The Ottawa Hospital, The University of Ottawa, Ottawa, ON, Canada*
[b] *Sorbonne Université, Institut des Sciences du Calcul et des Données, Department of Radiology, Tenon Hospital — HUEP — APHP, 4 rue de la Chine, 75020 Paris, France*

KEYWORDS
Renal cell carcinoma;
Angiomyolipoma;
Computed tomography (CT);
Magnetic resonance imaging (MRI);
Tumor characterization

Abstract Diagnosis of renal cell carcinomas (RCC) subtypes on computed tomography (CT) and magnetic resonance imaging (MRI) is clinically important. There is increased evidence that confident imaging diagnosis is now possible while standardization of the protocols is still required. Fat-poor angiomyolipoma show homogeneously increased unenhanced attenuation, homogeneously low signal on T2-weighted MRI and apparent diffusion coefficient (ADC) map, may contain microscopic fat and are classically avidly enhancing. Papillary RCC are also typically hyperattenuating and of low signal on T2-weighted MRI and ADC map; however, their gradual progressive enhancement after intravenous administration of contrast material is a differentiating feature. Clear cell RCC are avidly enhancing and may show intracellular lipid; however, these tumors are heterogeneous and are of characteristically increased signal on T2-weighted MRI. Oncocytomas and chromophobe tumors (collectively oncocytic neoplasms) show intermediate imaging findings on CT and MRI and are the most difficult subtype to characterize accurately; however, both show intermediately increased signal on T2-weighted with more gradual enhancement compared to clear cell RCC. Chromophobe tumors tend to be more homogeneous compared to oncocytomas, which can be heterogeneous, but other described features (e.g. scar, segmental enhancement inversion) overlap considerably between tumors. Tumor

* Corresponding author.
E-mail address: francois.cornelis@aphp.fr (F.H. Cornelis).

https://doi.org/10.1016/j.diii.2018.03.004

Please cite this article in press as: Schieda N, et al. Characterization of small (<4 cm) solid renal masses by computed tomography and magnetic resonance imaging: Current evidence and further development. Diagnostic and Interventional Imaging (2018), https://doi.org/10.1016/j.diii.2018.03.004

grade is another important consideration in small solid renal masses with emerging studies on both CT and MRI suggesting that high grade tumors may be separated from lower grade disease based upon imaging features.

Introduction

Small renal masses are commonly incidentally discovered on computed tomography (CT) and magnetic resonance imaging (MRI) examinations [1]. Once a small renal mass is characterized as enhancing (i.e. shown to be solid instead of cystic), the presumptive diagnosis becomes renal cell carcinoma (RCC). Those malignant tumors represent 80% of <4 cm solid renal masses in large surgical series [2,3]. Approximately 20% of <4 cm solid renal masses are benign, namely renal oncocytomas and fat-poor angiomyolipomas (AML) [3—5]. Differentiating between RCC and benign <4 cm solid renal masses is thus highly desirable to optimize treatment. Moreover, RCC show variable behavior depending on their subtype with clear cell RCC being the most aggressive compared to papillary RCC and the least aggressive variant chromophobe RCC [6—8]. Surveillance of small renal masses is now becoming a popular option in clinical practice since the risk of metastatic disease from renal masses <4 cm is low [8—12]. However, surveillance of clear cell and potentially other high grade small RCCs may occasionally yield unfavorable outcomes. Therefore, subtyping of RCCs and potentially providing information on anticipated grade are pathological features, which would be desirable to be extracted from imaging data.

This review article presents the established and emerging literature regarding the capabilities of both CT and MRI to differentiate between benign and malignant small renal masses, subtypes among the various RCC categories and also predict histological grade of disease [12—27].

Computed tomography

CT is the mainstay for the primary assessment of indeterminate renal masses [28]. CT is highly accurate to differentiate solid masses from simple and complex cysts by noting enhancement within a mass and absence of enhancement within a cyst. On conventional CT, enhancement is considered present when there is a >20 Hounsfield unit (HU) difference in attenuation of a mass comparing non-contrast enhanced CT (NECT) and contrast-enhanced CT (CECT) images [29,30]. Pitfalls in the CT evaluation of renal masses have been previously described [29]; however, there are two notable exceptions which merit discussion. Pseudoenhancement, which is the artificial increase in attenuation of a cyst on CECT compared to NECT images, can result in the misclassification of a cyst as a solid mass on CT [29,31]. Pseudoenhancement tends to occur more commonly in small endophytic masses [29] and is thought to be related to inadequate algorithmic correction of beam hardening artifacts from iodine [29,31]. Typically, when pseudoenhancement is suspected, an MRI can be performed to confirm the presence or absence of enhancement within a lesion [29]. More recently, it has been shown that dual-energy (DE) CT can effectively eliminate pseudoenhancement in renal masses through the use of higher keV monoenergetic images or iodine overlay images due to better correction of beam hardening effects [29,32] (Fig. 1). Not all solid tumors show a >20 HU difference in attenuation comparing NECT to CECT images and a substantial proportion of papillary RCC will not meet this threshold for enhancement at multiphase CT [29]. Most of these tumors will show intermediate range enhancement (between 10 or 15 and 20 HU difference) and can be further characterized with MRI (Fig. 2) [29]. DE-CT has also been recently preliminarily shown to be more sensitive for detection of enhancement using 70 keV images or through the use of iodine overlay data and iodine concentration measurements compared to attenuation measurement (Fig. 2) [29,33]; however, further study into this topic is required.

Non-enhanced computed tomography

On NECT, characterization of small renal masses relies predominantly on the detection of bulk or macroscopic fat, calcification and the baseline density of a mass. A small renal mass containing bulk or macroscopic fat can be confidently diagnosed as a renal angiomyolipoma [34]. The presence of bulk fat in RCC is rare [34]. Calcifications occur sporadically in RCC, generally does not occur in angiomyolipoma (AML) [34] and may occur in renal oncocytoma [35], therefore presence of calcification is useful to exclude the diagnosis of fat-poor AML only. Baseline attenuation of a renal mass at NECT has been investigated in fat-poor AML as a potential discriminating feature from RCC because the smooth muscle predominance of fat-poor AML should result in higher baseline attenuation (Fig. 3) [12,36]. It has been shown repeatedly that higher attenuation in a small renal mass at NECT is a feature of fat-poor AML; however, as a stand-alone feature, density is insufficient for diagnosis due to unacceptable overlap in attenuation values with RCC [13]. When the density of a homogeneous renal mass at NECT exceeds 70 HU, a diagnosis of a hemorrhagic cyst can be confidently established [28,29,37].

Contrast-enhanced computed tomography

At multi-phase CECT, enhancement pattern can be used to discriminate clear cell from papillary RCC with the former showing avid enhancement with washout of iodine and the latter showing gradual progressive enhancement

Please cite this article in press as: Schieda N, et al. Characterization of small (<4 cm) solid renal masses by computed tomography and magnetic resonance imaging: Current evidence and further development. Diagnostic and Interventional Imaging (2018), https://doi.org/10.1016/j.diii.2018.03.004

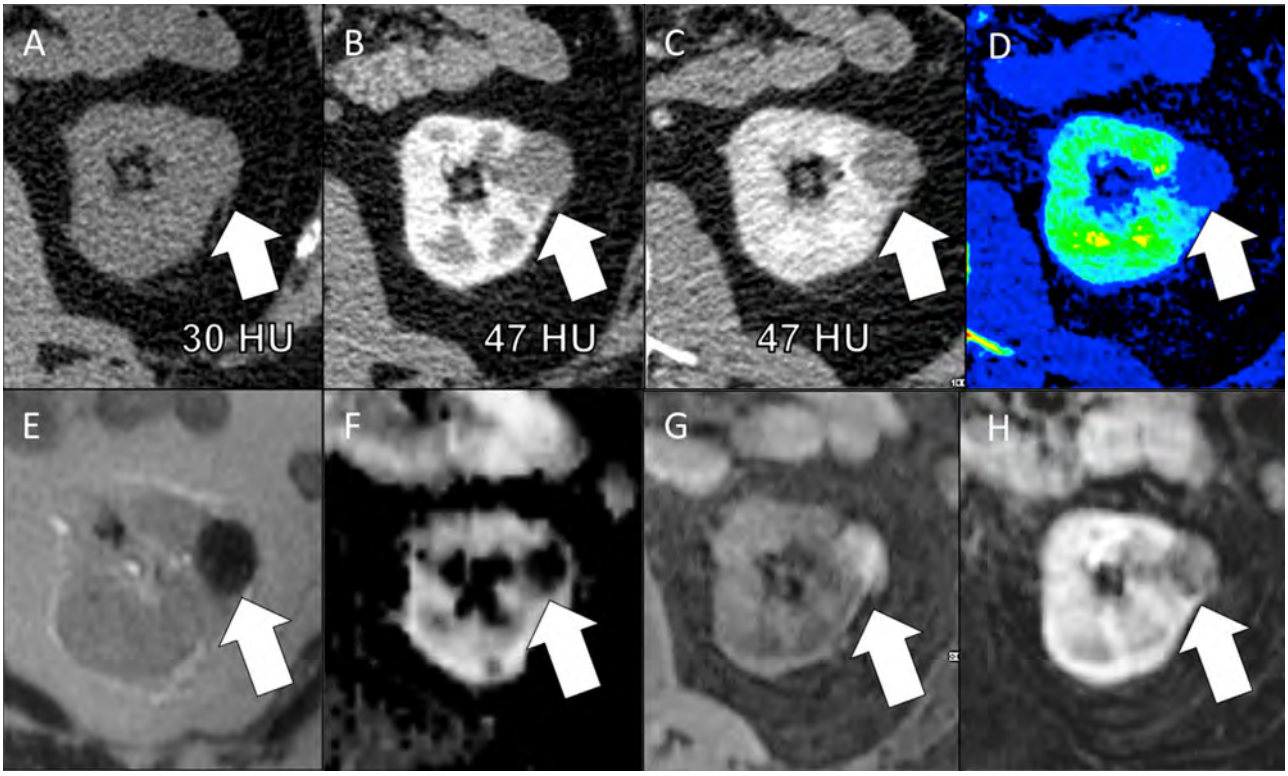

Figure 1. 61-year-old man with left upper pole indeterminate mass detected on ultrasound (not shown). Multiphase renal mass protocol CT was performed for further characterization. Axial non-contrast enhanced CT image (A) shows a homogeneous mass in the upper pole of the left kidney (white arrow) with attenuation value of 30 HU. The mass shows an increase in attenuation on axial corticomedullary phase (B) and nephrographic phase (C) contrast enhanced CT images which is in the indeterminate range for enhancement. Axial color iodine-overlay image (D) obtained from 70 keV rapid-kVp-switch dual-energy CT at the same level shows no iodine within the mass. Quantitative analysis showed iodine concentration of 0.3 mg/mL which is below previously described thresholds of enhancement. A diagnosis of hemorrhagic cyst was confidently established without proceeding to MRI and confirmed on follow-up examinations (not shown).

[12,16,29,38]. Using DECT, Mileto et al. also demonstrated that iodine concentration was significantly higher in clear cell compared to papillary tumors (Fig. 4) [39]. Fat-poor AML and oncocytic neoplasms also show avid enhancement and enhancement pattern alone is not sufficient to discriminate between renal masses on CT or MRI. It is important to emphasize that when designing a dedicated renal mass multi-phase CT protocol, a nephrographic phase (generally around 120 s) is required to optimally discriminate between renal masses and renal parenchyma and to maximize detection of enhancement in papillary RCC [16,28,29].

CT texture analysis

Various authors have investigated the role of CT texture analysis for diagnosis of renal mass subtypes. Previous studies have shown that fat-poor AML are more homogeneous, both subjectively and quantitatively, compared to RCC [23,29,40]. Clear cell RCC has also been shown to be more heterogeneous at texture analysis compared to papillary tumors [12,15,40]. Further development in this field is required.

Magnetic resonance imaging

T2-weighted MRI

T2-weighted (T2W) MRI has been suggested as the first imaging sequence to be used in the initial assessment of small solid renal masses for potential MRI subtyping [41]. On T2-weighted MRI, fat-poor AML (due to their intrinsically high smooth muscle content) (Fig. 5) and papillary RCC (due to their papillary projections and internal hemorrhagic contents) (Fig. 6) both show low signal intensity [22,42—44], which differ significantly from clear cell RCC (Fig. 7) and oncocytic neoplasms (Figs. 8 and 9) which are high to intermediate signal on T2W MRI [42,45]. T2W MRI is highly accurate to separate fat-poor AML and papillary RCC from clear cell RCC and oncocytic tumors and, when combined with other features can further separate the diagnoses with high degrees of accuracy [17]. T2W MRI is robust as it can be performed as a breath-hold single shot half-Fourier acquisition which is relatively insensitive to motion and rapidly acquired. Quantitative signal intensity ratios of renal masses compared to internal controls such as the renal cortex have been described [17,46,47]; however, generally subjective evaluation is more reproducible than quantitative

Please cite this article in press as: Schieda N, et al. Characterization of small (<4 cm) solid renal masses by computed tomography and magnetic resonance imaging: Current evidence and further development. Diagnostic and Interventional Imaging (2018), https://doi.org/10.1016/j.diii.2018.03.004

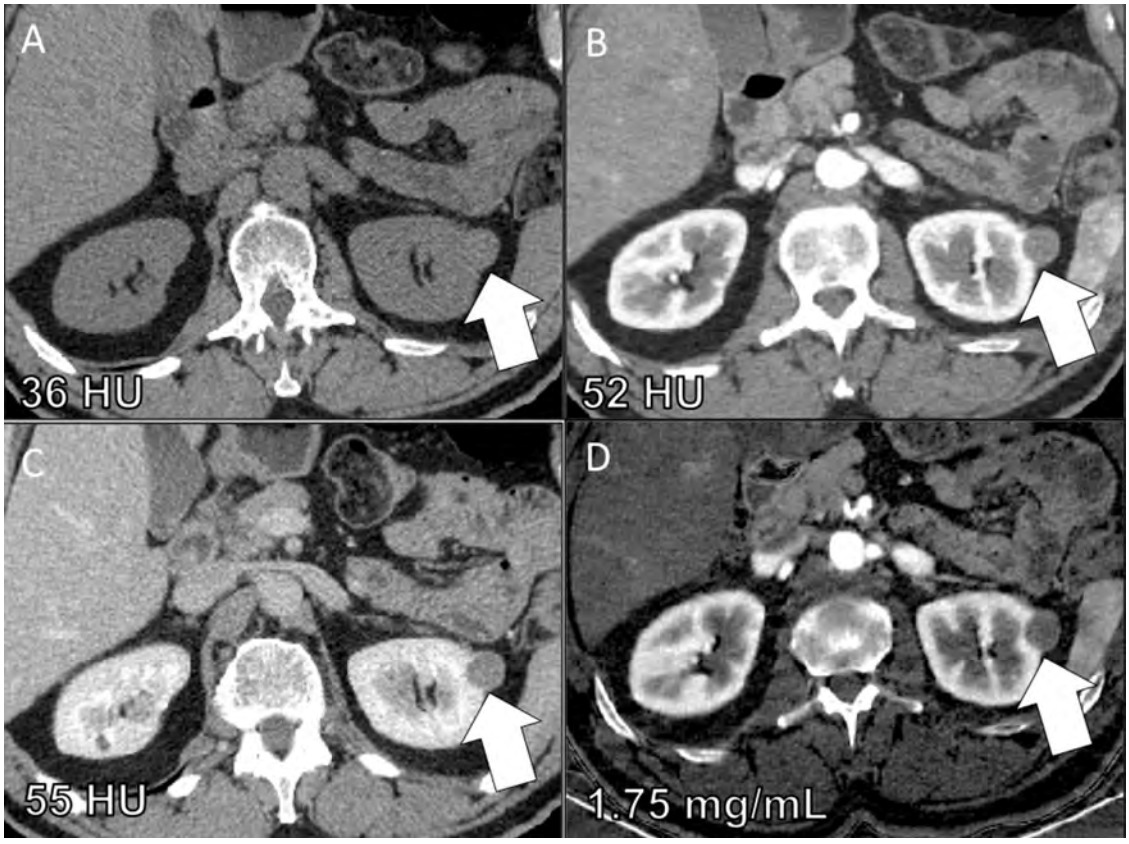

Figure 2. 54-year-old man with left upper pole indeterminate mass detected on single phase enhanced CT (not shown). Multi-phase renal mass protocol CT was performed for further characterization. Axial unenhanced CT image (A) shows a homogeneous mass in the upper pole of the left kidney (white arrow) with an attenuation value of 36 HU. The mass shows an increase in attenuation on axial corticomedullary phase (B) and nephrographic phase (C) CT images which his in the indeterminate range for enhancement. Axial iodine-overlay image (D) obtained from 70 keV rapid-kVp-switch dual energy CT at the same level shows low level density within the mass and quantitative analysis showed iodine concentration of 1.75 mg/mL which is above the 1.3 mg/mL threshold described by Zarzour et al. to differentiate renal cell carcinoma (RCC) from hemorrhagic cyst. A diagnosis of papillary RCC was established at percutaneous biopsy.

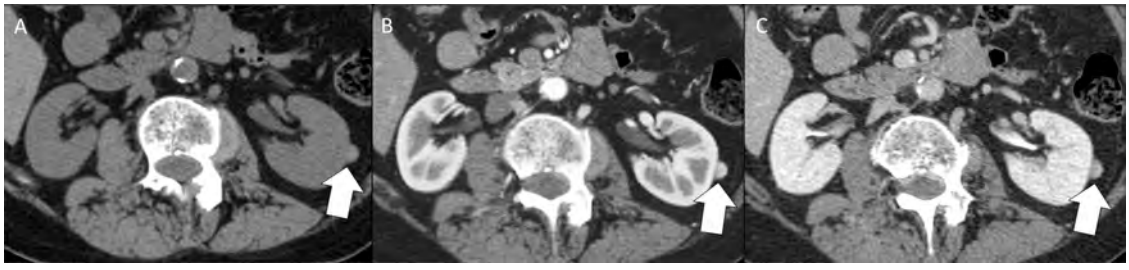

Figure 3. 55-year-old woman with small fat-poor angiomyolipoma in the left kidney interpolar region. The tumor was identified on multi-phase CT performed to rule out vasculitis. Axial NECT image (A) shows a homogeneously hyperattenuating nodule in the interpolar region of the left kidney (white arrow) measuring 52 HU. The mass shows avid enhancement on axial corticomedullary phase (B) and washes out contrast on nephrographic phase (C) CECT images. The mass was reported as most likely representing an RCC and was resected with final pathology compatible with a smooth muscle predominant AML.

analysis across institutions [48]. MR imaging of oncocytoma may show high signal intensity on T2-weighted MRI compared to renal cortex and may demonstrate a central scar which is typically of low signal intensity and shows homogeneous enhancement after intravenous administration of a gadolinium chelate.

Dynamic gadolinium chelate enhanced MRI

Epithelial tumor enhancement present similar features on MRI as CT and give useful information when trying to distinguish subtypes of RCC. The clear cell RCCs usually present with intense and rapid enhancement (Fig. 7), during the

Please cite this article in press as: Schieda N, et al. Characterization of small (<4 cm) solid renal masses by computed tomography and magnetic resonance imaging: Current evidence and further development. Diagnostic and Interventional Imaging (2018), https://doi.org/10.1016/j.diii.2018.03.004

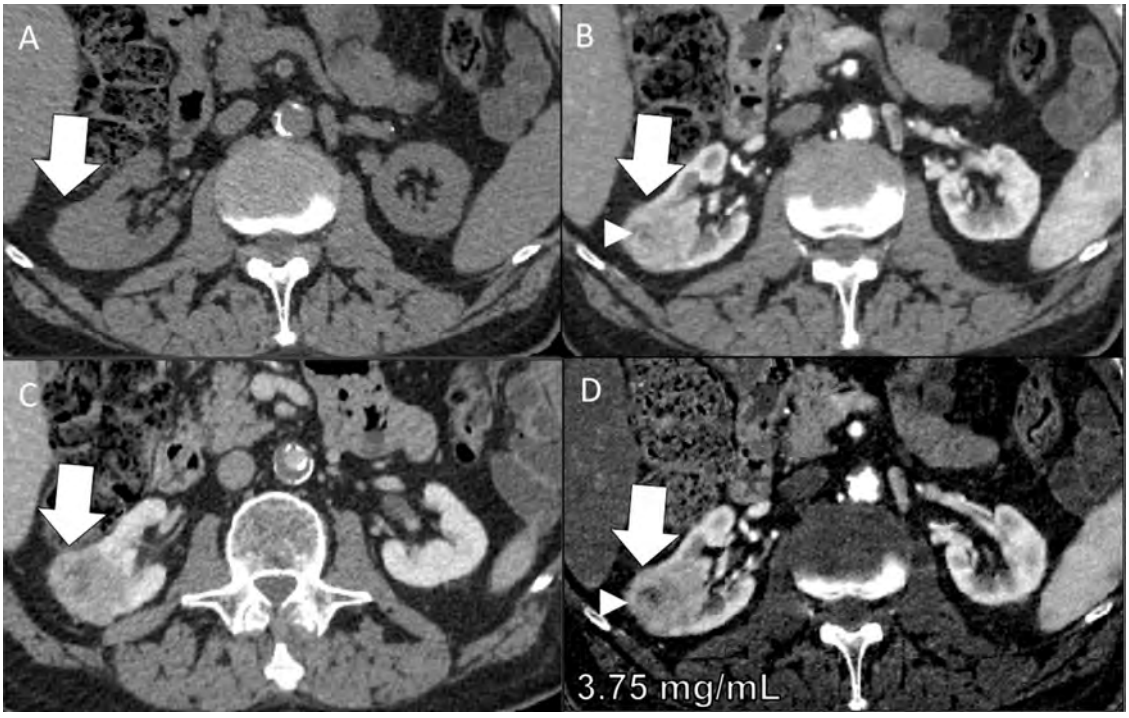

Figure 4. 84-year-old man with suspicious renal mass detected on ultrasound performed at another facility. Multi-phase renal mass protocol CT was performed for further characterization. Axial NECT image (A) shows a heterogeneous mass in the interpolar region of the right kidney (white arrow). The mass shows avid heterogeneous enhancement on axial corticomedullary phase (B) and washout of contrast on the nephrographic phase (C) CECT images. Axial iodine-overlay image (D) obtained from 70 keV rapid-kVp-switch DECT at the same level shows marked iodine uptake within the mass measuring 3.75 mg/mL. There is a central non-enhancing portion within the mass which may reflect necrosis. Biopsy confirmed clear cell RCC.

cortimedullary and nephrographic phases, which help to differentiate clear cell tumors from the lower enhancement of papillary RCC (Fig. 6) and chromophobe RCC (Fig. 8) [24]. On later phases, clear cell RCC shows rapid washout of contrast, appearing hypointense to the renal cortex by the excretory phase. Moreover, because of areas of necrosis, clear cell RCC enhancement is often heterogeneous. Fat-poor AML also commonly show avid early enhancement with washout kinetics at contrast-enhanced CT and MRI (Fig. 5) [12]. This enhancement pattern overlaps with clear-cell RCC and chromophobe tumors but differs from papillary RCC, which typically show a gradual progressive wash-in enhancement pattern [24].

T1-weighted dual-echo chemical shift MRI

Kim et al. first described the use of chemical shift MRI as a potential diagnostic tool for fat-poor AML as they reported that scattered fat cells result in a signal drop on opposed-phase (OP) compared to in-phase (IP) images [49]. Later, Outwater et al. showed that clear cell RCC also characteristically lose signal on OP chemical shift MRI due to the presence of intracellular lipid molecules [50]. It is now understood that signal loss on OP MRI can occur to some degree in nearly all renal tumors [51,52]; however, most commonly and to the greatest extent in clear cell RCC (Fig. 7) and fat-poor AML [51]. Therefore, a substantial signal intensity drop on OP MRI among T2W hyperintense renal masses would favor a clear cell RCC over an oncocytic neoplasm and among hypointense renal masses on T2W images would favor a diagnosis of fat-poor AML over papillary RCC [12]. The utility of this imaging finding in practice is limited because not all clear cell RCC will show signal drop on OP MRI and only a minority of fat-poor AML demonstrate this finding [47,53].

A signal intensity drop on IP compared to OP images (due to the susceptibility artifact) is an imaging finding that is described in RCC, most commonly papillary tumors due to chronic hemorrhage and hemosiderin deposition [22,43]. This finding is not encountered in fat-poor AML which do not hemorrhage [22]. Similarly, an acutely hemorrhagic small renal mass showing high signal on fat suppressed T1W gradient recalled echo images would favor a diagnosis of RCC [28,54].

Diffusion-weighted imaging

As proposed in prostate carcinoma [55,56], DWI helps to establish the aggressiveness of clear-cell RCCs [57]. A decreasing trend of ADC values was observed with increasing Fuhrman nuclear grade [58]. Higher ADC values for low-grade tumors (Fuhrman grade $\leq$2) have been reported compared to high grade tumors (Fuhrman grade $\geq$3) [57]. The mean ADC of high grade RCC has also been reported to be significantly lower than low grade tumors [58]. The ADC value of papillary RCCs (Fig. 6) may be also discriminant with lower reported values of ADC compared to other renal tumors such as oncocytomas or clear-cell RCCs [24,59]. Limitations of DWI exist; however, in that quantitative assessment may not be reproducible across MR systems

Please cite this article in press as: Schieda N, et al. Characterization of small (<4 cm) solid renal masses by computed tomography and magnetic resonance imaging: Current evidence and further development. Diagnostic and Interventional Imaging (2018), https://doi.org/10.1016/j.diii.2018.03.004

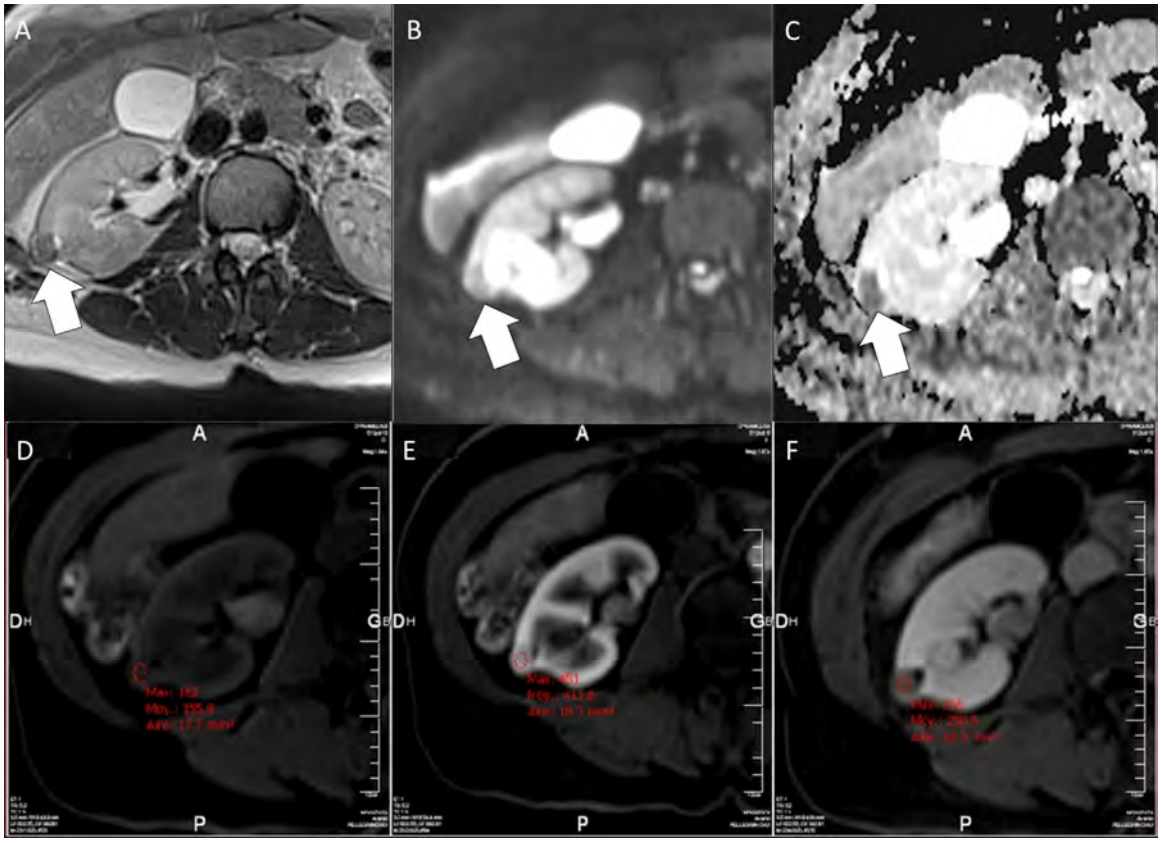

Figure 5. 42-year-old woman with small fat-poor angiomyolipoma in the right kidney. The tumor was identified incidentally on CT (not showed). Axial T2-weighted MR image (A) shows a homogeneous low signal intensity nodule (white arrow). The mass presented low signal intensity on DWI (C) and low ADC values on ADC map (D). The mass is isointense on T1-weighted MR image before intravenous administration of a gadolinium chelate (D), the mass shows avid enhancement on axial T1W MR image (E) and washes out contrast on nephrographic phase (F).

and institutions and are subject to the variable b values used. AML also have low ADC values (Fig. 5) which overlap considerably with papillary RCC [12].

Multi-parametric MRI approach to diagnosis of small renal masses

Imaging features of the most common renal tumors differ on multiparametric MRI (Table 1). A standardized step-by-step approach to the images helps to differentiate a particular tumor subtype from another and to standardize reporting [60]. We recently proposed an algorithm based on: (1) T2w images, (2) Dual echo chemical shift MRI; (3) DWI; (4) wash-in analysis of DCE-images; and (5) wash-out analysis of DCE images [60]. T2W images help distinguish between fat-poor AML and papillary RCC, which are characteristically of low T2w signal intensity from the other tumors [24,46,61—66]. Clear cell RCC and fat poor AML may show a signal drop on out-phase sequences whereas it is not reported for oncocytoma [24,27,46,67]. This signal drop may be sporadically observed in chromophobe RCC [64,68] or papillary RCC [44]; however, tends to be less when compared to clear cell RCC and fat poor AML. Low ADC is often observed for AML and papillary RCC while ADC remains heterogeneous but often high for oncocytomas and clear cell RCC [24,57,59,69—71]. Akin to T2w imaging, chromophobe RCC presents a slightly low ADC compared to these 2 last subtypes. Finally, the analysis of DCE is critical to formulate an imaging diagnosis [24,27,46,72—74]. Clear cell RCC as well as fat poor AML present a rapid and intense enhancement during the corticomedullary phase, whereas, peak of enhancement is slightly delayed for oncocytoma and chromophobe RCC. For all of these tumor subtypes, a wash-out pattern of enhancement is observed over time. The enhancement is conversely progressive for papillary RCC. Canvaser et al. retrospectively reviewed 121 cT1a masses who underwent magnetic resonance imaging and partial or radical nephrectomy using a predefined algorithm [41]. Applying various thresholds of confidence using their algorithm achieved 78% sensitivity and 80% specificity and 95% sensitivity with 58% specificity. The use of probability scales or Likert scores when reporting multiparametric MRI in a standardized fashion may decrease the number of diagnostic renal mass biopsies and potentially the number of nephrectomies performed for benign diagnoses. Nevertheless, standardization of imaging protocols and reporting criteria is still needed to improve interobserver reliability and larger sample sizes or multi-institutional studies are desired to confirm accuracy.

Please cite this article in press as: Schieda N, et al. Characterization of small (<4 cm) solid renal masses by computed tomography and magnetic resonance imaging: Current evidence and further development. Diagnostic and Interventional Imaging (2018), https://doi.org/10.1016/j.diii.2018.03.004

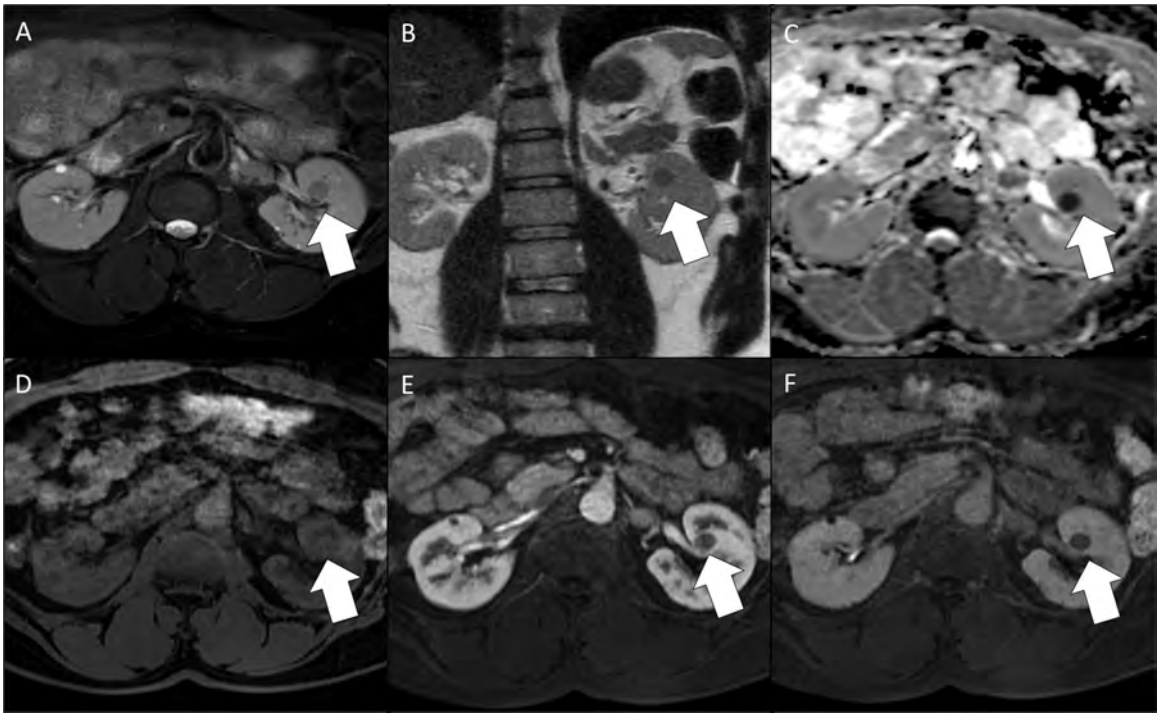

Figure 6. 52-year-old man with 12 mm papillary renal cell carcinoma in the left kidney. The tumor was identified incidentally on CT examination (not showed). Axial and coronal T2-weighted MR images (A and B) show a homogeneous low signal intensity nodule (white arrow). The mass has low ADC values on ADC map (C). The mass is isointense on T1-weighted MR image before intravenous administration of a gadolinium chelate (D), the mass shows progressive enhancement on axial T1-weighted image (E) without wash-out on nephrographic phase (F).

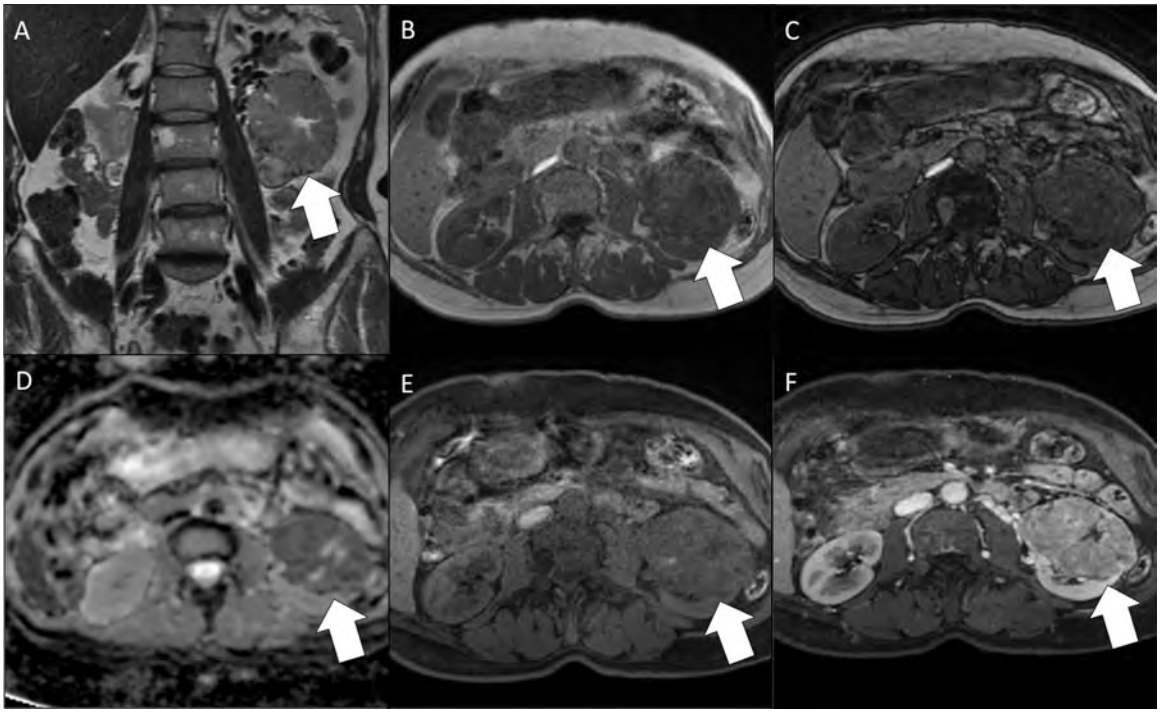

Figure 7. 65-year-old man with 77 mm clear cell RCC in the left kidney. The tumor was identified on ultrasound and CT examination (not shown). Coronal T2-weighted MR image (A) shows a heterogeneous mid low signal intensity nodule with flow voids, central necrosis and a pseusocapsule (white arrow). The mass shows a mid-signal drop on dual chemical shift MR images (B and C) and low ADC values on ADC map (D). The mass is isointense on T1-weighted MR image before intravenous administration of a gadolinium chelate (E), the mass shows avid but heterogeneous enhancement on axial T1-weighted MR images (F).

Please cite this article in press as: Schieda N, et al. Characterization of small (<4 cm) solid renal masses by computed tomography and magnetic resonance imaging: Current evidence and further development. Diagnostic and Interventional Imaging (2018), https://doi.org/10.1016/j.diii.2018.03.004

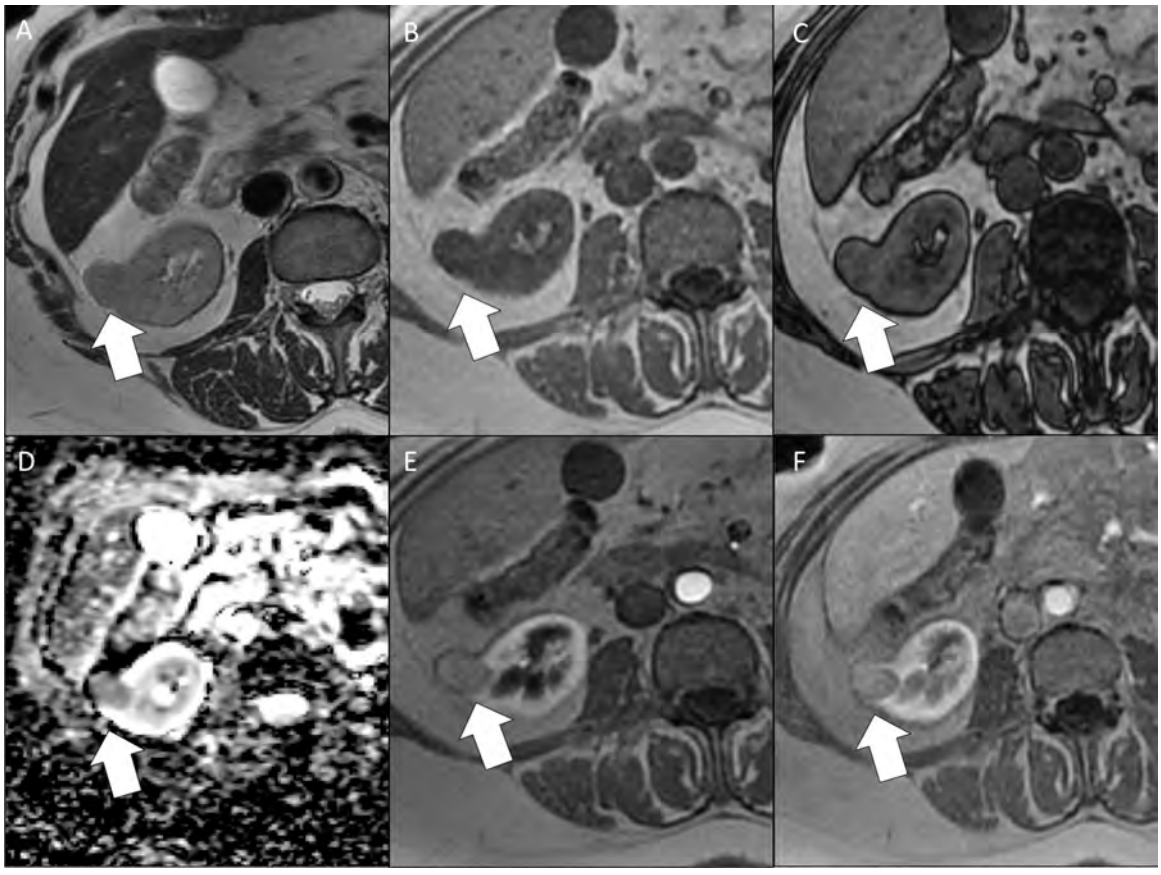

Figure 8. 61-year-old man with 25 mm chromophobe RCC in the right kidney. The tumor was identified on ultrasound examination (not showed). Axial T2-weighted MR image (A) shows a homogeneous mid low signal intensity nodule (white arrow). The mass displays no signal drop on dual chemical shift MR images (B and C) but low ADC values on ADC map (D). The mass is isointense on T1-weighted MR image before intravenous administration of a gadolinium chelate (E) and shows homogeneous but slightly delayed enhancement on axial T1-weighted MR image intravenous administration of a gadolinium chelate (F).

Other imaging findings

Other imaging findings in the characterization of small renal masses are generally not useful. Segmental enhancement inversion (SEI) though initially described as being a specific finding for oncocytoma is very controversial [54,75] with limited utility on CT and MRI thus far [28,54,75]. The presence of a central scar also described as being a feature of oncocytoma [54]; can also be seen in RCC [28,38,64,74]. Using MRI, Rosenkrantz et al. observed similar features in oncocytomas and chromophobe RCC [68]. Galmiche et al. demonstrated that oncocytomas present significantly higher ADC ($P = 0.002$) and faster enhancement ($P = 0.007—0.012$) but lower SII ($P = 0.03$) than chromophobe RCC [74]. This combination provided sensitivity of 92.3% (24/26), specificity of 93.8% (15/16), and accuracy of 92.9% (39/42) for the diagnosis of oncocytomas.

A variety of growth patterns have been described in renal masses on imaging, a recent study showed that a substantial amount of exophytic growth (i.e. nearly entirely exophytic pattern) was associated with benign lesions; however, there was overlap between groups and other growth features were not useful [48].

Grading of renal cell carcinomas with CT and MRI

Grade of disease in RCC is an important predictor of aggressiveness. In clear cell RCC, the Fuhrman nuclear grading (FNG) system is used and has been validated to correspond with adverse patient outcomes including metastatic disease and survival [6,76]. Grading of papillary RCC with the Type 1/Type 2 classification system and chromophobe RCC with the Chromophobe tumor grading system is more controversial; however, has also been shown to be useful to some extent as they are both associated with adverse patient outcomes [6,20,28]. In small renal masses, grade may be an important parameter to consider particularly if a patient is being enrolled in active surveillance. Histological grading of RCC at percutaneous biopsy can be performed, but is generally not considered accurate due to sampling issues and a substantial proportion of tumors will have their histological grade altered after nephrectomy when compared to biopsy [8,77]. The use of CT or MRI to predict grade of disease is therefore desirable. Both CT and MRI parameters including enhancement pattern, DWI metrics and texture analysis have been shown to correlate with the FNG system,

Please cite this article in press as: Schieda N, et al. Characterization of small (<4 cm) solid renal masses by computed tomography and magnetic resonance imaging: Current evidence and further development. Diagnostic and Interventional Imaging (2018), https://doi.org/10.1016/j.diii.2018.03.004

Table 1 Evocative MR features reported in the literature of the most common renal tumors (adapted from [60]).

Tumor subtype	AML	AML without visible fat	Renal oncocytoma	Clear cell RCC	Papillary RCC	Chromophobe RCC	References
% in surgical series	2—6		3—7	75—80	10—15	5	[79]
T2-weighted	Heterogeneous with high signal intensity	Low signal intensity	Heterogeneous Central area (scar)	Heterogeneous Central area (necrosis) Pseudocapsule Vascular invasion Vascular signal void	Homogeneous Low signal intensity Pseudocapsule	Mid Heterogeneity Central area (necrosis)	[24,46,61—66]
T1-weighted	Heterogeneous with high signal intensity	—	—	Heterogeneous High signal intensity of central area	—	—	[46,68]
Fat saturation	Signal suppression	—	—	Small area with signal suppression	—	—	[67]
Dual chemical shift MRI	Interface	Signal drop (Out-phase)	No	Signal drop Interface	Signal drop (in-phase)	No	[24,27,46,67]
DCE-MRI	Heterogeneous	Avid arterial enhancement	Heterogeneous Moderate wash-in and wash-out	Heterogeneous Avid arterial wash-in and quick wash-out	Slow enhancement	Moderate wash-in and wash-out	[24,27,46,72,73]
Late post-contrast T1-weighted	—	—	Complete late segmental inversion of central scar	Absence of segmental inversion of necrosis	—	Absence of segmental inversion of necrosis	[64]
DWI	—	Low ADC	—	Heterogeneous	Low ADC	—	[24,57,59,69—71,74]

Please cite this article in press as: Schieda N, et al. Characterization of small (<4cm) solid renal masses by computed tomography and magnetic resonance imaging: Current evidence and further development. Diagnostic and Interventional Imaging (2018), https://doi.org/10.1016/j.diii.2018.03.004

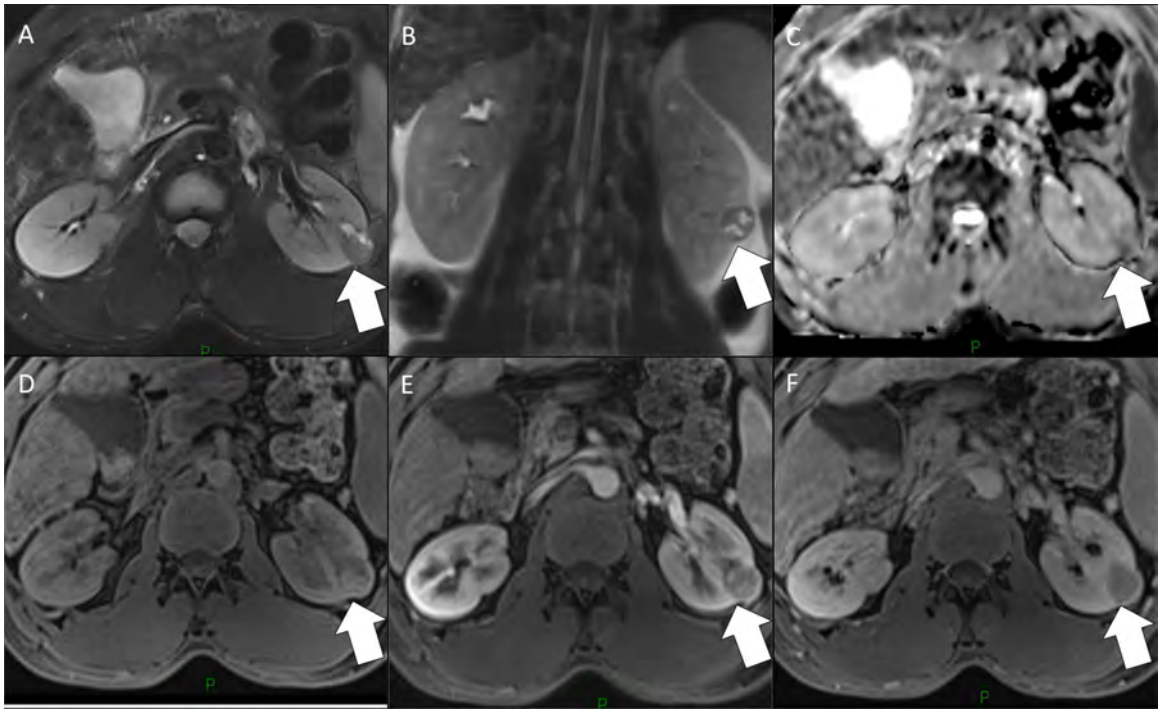

Figure 9. 47-year-old man with 25 mm oncocytoma in the left kidney. The tumor was identified incidentally on CT examination (not shown). Axial and coronal T2-weighted MR images (A and B) show homogeneous low signal intensity nodule with central area (white arrow). The mass displays heterogeneous ADC values on ADC map (C). The mass is isointense on T1-weighted MR image before intravenous administration of a gadolinium chelate (D), the mass shows avid heterogeneous enhancement on axial T1-weighted MR image (E) and washes out contrast on nephrographic phase with slight enhancement of the central area (F).

Type 1 versus Type 2 and more recently the Chromophobe tumor grading system in clear cell, papillary and chromophobe RCC respectively [8,20,78]. Future larger scale studies are required to determine reproducibility of these findings which have been only reported in single institution retrospective analyses to date and how they can be incorporated into CT or MRI decision tree algorithms which are used to diagnose a subtype of tumor encountered on imaging.

Conclusion

In conclusion, CT is highly accurate for differentiation of solid from cystic masses and accuracy is improved using dual-energy techniques to overcome the pitfall of pseudoenhancement with preliminary data suggesting it may also have increased sensitivity for detection of enhancement in papillary RCC which are characteristically hypoenhancing. Fat-poor AML can be diagnosed with a high degree of accuracy when encountered in women and appearing homogeneously hyperattenuating on CT, hypointense on T2W and ADC map and showing avid enhancement. Clear cell RCC and oncocytic neoplasms (oncocytoma and chromophobe RCC) are hyperintense on T2W MRI; however, degree of corticomedullary enhancement is higher in clear cell tumors which may be a distinguishing feature. Grade of RCC is an important prognostic factor which may not be accurately reflected in biopsy specimens and preliminary data suggest that both CT and MRI features may be useful to differentiate between low and high-grade disease. Multicentric clinical trials are now required to validate these results. Further developments such standardization of the data collection and analysis using newly developed radiomics techniques would help to better identify the renal tumor subtypes.

Disclosure of interest

The authors declare that they have no competing interest.

References

[1] Heilbrun ME, Remer EM, Casalino DD, Beland MD, Bishoff JT, Blaufox MD, et al. ACR appropriateness criteria indeterminate renal mass. J Am Coll Radiol 2015;12:333—41.
[2] Violette P, Abourbih S, Szymanski KM, Tanguay S, Aprikian A, Matthews K, et al. Solitary solid renal mass: can we predict malignancy? BJU Int 2012;110(Pt B):E548—52.
[3] Frank I, Blute ML, Cheville JC, Lohse CM, Weaver AL, Zincke H. Solid renal tumors: an analysis of pathological features related to tumor size. J Urol 2003;170(Pt 1):2217—20.
[4] Fujii Y. Benign lesions at surgery for presumed renal cell carcinoma: an Asian perspective. Int J Urol 2010;17:500.
[5] Park SY, Jeon SS, Lee SY, Jeong BC, Seo SI, Lee HM, et al. Incidence and predictive factors of benign renal lesions in Korean patients with preoperative imaging diagnoses of renal cell carcinoma. J Korean Med Sci 2011;26:360—4.
[6] Paner GP, Amin MB, Alvarado-Cabrero I, Young AN, Stricker HJ, Moch H, et al. A novel tumor grading scheme for chromophobe renal cell carcinoma: prognostic utility and comparison with Fuhrman nuclear grade. Am J Surg Pathol 2010;34:1233—40.
[7] Steffens S, Janssen M, Roos FC, Becker F, Schumacher S, Seidel C, et al. Incidence and long-term prognosis of papillary compared to clear cell renal cell carcinoma: a multicentre study. Eur J Cancer 2012;48:2347—52.

Please cite this article in press as: Schieda N, et al. Characterization of small (<4 cm) solid renal masses by computed tomography and magnetic resonance imaging: Current evidence and further development. Diagnostic and Interventional Imaging (2018), https://doi.org/10.1016/j.diii.2018.03.004

[8] Lim RSMM, Krishna S, Shbana W, Lavallee L, Flood T, Schieda N. Diagnostic accuracy of unenhanced computed tomography (CT) analysis to differentiate low-grade from high-grade chromophobe renal cell carcinoma. Chicago, IL, USA: Radiological Society of North America (RSNA); 2017.
[9] Campbell SC, Novick AC, Belldegrun A, Blute ML, Chow GK, Derweesh IH, et al. Guideline for management of the clinical T1 renal mass. J Urol 2009;182:1271—9.
[10] Flum AS, Hamoui N, Said MA, Yang XJ, Casalino DD, McGuire BB, et al. Update on the diagnosis and management of renal angiomyolipoma. J Urol 2016;195(P1):834—46.
[11] Silverman SG, Israel GM, Herts BR, Richie JP. Management of the incidental renal mass. Radiology 2008;249:16—31.
[12] Lim RS, Flood TA, McInnes MDF, Lavallee LT, Schieda N. Renal angiomyolipoma without visible fat: can we make the diagnosis using CT and MRI? Eur Radiol 2017.
[13] Schieda N, Hodgdon T, El-Khodary M, Flood TA, McInnes MD, Unenhanced CT. for the diagnosis of minimal-fat renal angiomyolipoma. AJR Am J Roentgenol 2014;203:1236—41.
[14] Yang CW, Shen SH, Chang YH, Chung HJ, Wang JH, Lin AT, et al. Are there useful CT features to differentiate renal cell carcinoma from lipid-poor renal angiomyolipoma? AJR Am J Roentgenol 2013;201:1017—28.
[15] Takahashi N, Leng S, Kitajima K, Gomez-Cardona D, Thapa P, Carter RE, et al. Small (<4 cm) Renal masses: differentiation of angiomyolipoma without visible fat from renal cell carcinoma using unenhanced and contrast-enhanced CT. AJR Am J Roentgenol 2015;205:1194—202.
[16] Lee-Felker SA, Felker ER, Tan N, Margolis DJ, Young JR, Sayre J, et al. Qualitative and quantitative MDCT features for differentiating clear cell renal cell carcinoma from other solid renal cortical masses. AJR Am J Roentgenol 2014;203:W516—24.
[17] Schieda N, Dilauro M, Moosavi B, Hodgdon T, Cron GO, McInnes MD, et al. MRI evaluation of small (<4 cm) solid renal masses: multivariate modeling improves diagnostic accuracy for angiomyolipoma without visible fat compared to univariate analysis. Eur Radiol 2016;26:2242—51.
[18] Schieda N, Thornhill RE, Al-Subhi M, McInnes MD, Shabana WM, van der Pol CB, et al. Diagnosis of sarcomatoid renal cell carcinoma with CT: evaluation by qualitative imaging features and texture analysis. AJR Am J Roentgenol 2015;204:1013—23.
[19] Schieda N, Vakili M, Dilauro M, Hodgdon T, Flood TA, Shabana WM. Solid renal cell carcinoma measuring water attenuation (−10 to 20 HU) on unenhanced CT. AJR Am J Roentgenol 2015;205:1215—21.
[20] Young JR, Coy H, Douek M, Lo P, Sayre J, Pantuck AJ, et al. Type 1 papillary renal cell carcinoma: differentiation from Type 2 papillary RCC on multiphasic MDCT. Abdom Radiol 2017;42:1911—8.
[21] Young JR, Margolis D, Sauk S, Pantuck AJ, Sayre J, Raman SS. Clear cell renal cell carcinoma: discrimination from other renal cell carcinoma subtypes and oncocytoma at multiphasic multidetector CT. Radiology 2013;267:444—53.
[22] Murray CA, Quon M, McInnes MD, van der Pol CB, Hakim SW, Flood TA, et al. Evaluation of T1-weighted MRI to detect intratumoral hemorrhage within papillary renal cell carcinoma as a feature differentiating from angiomyolipoma without visible fat. AJR Am J Roentgenol 2016;207:585—91.
[23] Hodgdon T, McInnes MDF, Schieda N, Flood TA, Lamb L, Thornhill RE, Can Quantitative CT. Texture analysis be used to differentiate fat-poor renal angiomyolipoma from renal cell carcinoma on unenhanced CT images? Radiology 2015;276:787—96.
[24] Cornelis F, Tricaud E, Lasserre AS, Petitpierre F, Bernhard JC, Le Bras Y, et al. Routinely performed multiparametric magnetic resonance imaging helps to differentiate common subtypes of renal tumours. Eur Radiol 2014;24:1068—80.
[25] Cornelis F, Tricaud E, Lasserre AS. Multiparametric magnetic resonance imaging for the differentiation of low and high grade clear cell renal carcinoma. Eur Radiol 2015;25:24.
[26] Kim JK, Park S-Y, Shon J-H, Cho K-S. Angiomyolipoma with minimal fat: differentiation from renal cell carcinoma at biphasic helical CT. Radiology 2004;230:677—84.
[27] Hindman N, Ngo L, Genega EM, Melamed J, Wei J, Braza JM, et al. Angiomyolipoma with minimal fat: can it be differentiated from clear cell renal cell carcinoma by using standard MR techniques? Radiology 2012;265:468—77.
[28] Kang SK, Huang WC, Pandharipande PV, Chandarana H. Solid renal masses: what the numbers tell us. AJR Am J Roentgenol 2014;202:1196—206.
[29] Krishna S, Murray CA, McInnes MD, Chatelain R, Siddaiah M, Al-Dandan O, et al. CT imaging of solid renal masses: pitfalls and solutions. Clin Radiol 2009;72:708—21.
[30] Israel GM, Bosniak MA, How I. Do it: evaluating renal masses. Radiology 2005;236:441—50.
[31] Israel GM, Bosniak MA. Pitfalls in renal mass evaluation and how to avoid them. Radiographics 2008;28:1325—38.
[32] Mileto A, Nelson RC, Paulson EK, Marin D. Dual-energy MDCT for imaging the renal mass. AJR Am J Roentgenol 2015;204:W640—7.
[33] Zarzour JG, Milner D, Valentin R, Jackson BE, Gordetsky J, West J, et al. Quantitative iodine content threshold for discrimination of renal cell carcinomas using rapid kV-switching dual-energy CT. Abdom Radiol (New York) 2017;42:727—34.
[34] Schieda N, Kielar AZ, Al Dandan O, McInnes MD, Flood TA. Ten uncommon and unusual variants of renal angiomyolipoma (AML): radiologic-pathologic correlation. Clin Radiol 2015;70:206—20.
[35] Wasserman NF, Ewing SL. Calcified renal oncocytoma. AJR Am J Roentgenol 1983;141:747—9.
[36] Jinzaki M, Silverman SG, Akita H, Nagashima Y, Mikami S, Oya M. Renal angiomyolipoma: a radiological classification and update on recent developments in diagnosis and management. Abdom Imaging 2014;39:588—604.
[37] Jonisch AI, Rubinowitz AN, Mutalik PG, Israel GM. Can high-attenuation renal cysts be differentiated from renal cell carcinoma at unenhanced CT? Radiology 2007;243:445—50.
[38] Low G, Huang G, Fu W, Moloo Z, Girgis S. Review of renal cell carcinoma and its common subtypes in radiology. World J Radiol 2015;8:484—500.
[39] Mileto A, Marin D, Alfaro-Cordoba M, Ramirez-Giraldo JC, Eusemann CD, Scribano E, et al. Iodine quantification to distinguish clear cell from papillary renal cell carcinoma at dual-energy multidetector CT: a multireader diagnostic performance study. Radiology 2014;273:813—20.
[40] Yan L, Liu Z, Wang G, Huang Y, Liu Y, Yu Y, et al. Angiomyolipoma with minimal fat: differentiation from clear cell renal cell carcinoma and papillary renal cell carcinoma by texture analysis on CT images. Acad Radiol 2015;22:1115—21.
[41] Canvasser NE, Kay FU, Xi Y, Pinho DF, Costa D, de Leon AD, et al. Diagnostic accuracy of multiparametric magnetic resonance imaging to identify clear cell renal cell carcinoma in cT1a renal masses. J Urol 2017;198:780—6.
[42] Ramamurthy NK, Moosavi B, McInnes MD, Flood TA, Schieda N, Multiparametric MRI. of solid renal masses: pearls and pitfalls. Clin Radiol 2015;70:304—16.
[43] Childs DD, Clingan MJ, Zagoria RJ, Sirintrapun J, Tangtiang K, Anderson A, et al. In-phase signal intensity loss in solid renal masses on dual-echo gradient-echo MRI: association with malignancy and pathologic classification. Am J Roentgenol 2014;203:W421—8.
[44] Schieda N, van der Pol CB, Moosavi B, McInnes MD, Mai KT, Flood TA. Intracellular lipid in papillary renal cell carcinoma (pRCC):

Please cite this article in press as: Schieda N, et al. Characterization of small (<4 cm) solid renal masses by computed tomography and magnetic resonance imaging: Current evidence and further development. Diagnostic and Interventional Imaging (2018), https://doi.org/10.1016/j.diii.2018.03.004

T2 weighted (T2W) MRI and pathologic correlation. Eur Radiol 2015;25:2134—42.
[45] Pedrosa I, Sun MR, Spencer M, Genega EM, Olumi AF, Dewolf WC, et al. MR imaging of renal masses: correlation with findings at surgery and pathologic analysis. RadioGraphics 2008;28:985—1003.
[46] Sasiwimonphan K, Takahashi N, Leibovich BC, Carter RE, Atwell TD, Kawashima A. Small (<4 cm) renal mass: differentiation of angiomyolipoma without visible fat from renal cell carcinoma utilizing MR imaging. Radiology 2012;263:160—8.
[47] Hakim SW, Schieda N, Hodgdon T, McInnes MD, Dilauro M, Flood TA. Angiomyolipoma (AML) without visible fat: ultrasound, CT and MR imaging features with pathological correlation. Eur Radiol 2016;26:592—600.
[48] Lim RSMM, Siddaiah M, Shabana W, Lavallee L, Flood T, Schieda N. Are growth patterns in small (<4 cm) solid renal masses useful for predicting benign histology? Chicago, IL, USA: Radiological Society of North America (RSNA) 2017; 2017.
[49] Kim JK, Kim SH, Jang YJ, Ahn H, Kim C-S, Park H, et al. Renal angiomyolipoma with minimal fat: differentiation from other neoplasms at double-echo chemical shift FLASH MR imaging. Radiology 2006;239:174—80.
[50] Outwater EK, Blasbalg R, Siegelman ES, Vala M. Detection of lipid in abdominal tissues with opposed-phase gradient-echo images at 1.5 T: techniques and diagnostic importance. Radiographics 1998;18:1465—80.
[51] Karlo CA, Donati OF, Burger IA, Zheng J, Moskowitz CS, Hricak H, et al. MR imaging of renal cortical tumours: qualitative and quantitative chemical shift imaging parameters. Eur Radiol 2013;23:1738—44.
[52] Schieda N, Avruch L, Flood TA. Small (<1 cm) incidental echogenic renal cortical nodules: chemical shift MRI outperforms CT for confirmatory diagnosis of angiomyolipoma (AML). Insights Imaging 2014;5:295—9.
[53] Jhaveri KS, Elmi A, Hosseini-Nik H, Hedgire S, Evans A, Jewett M, et al. Predictive value of chemical-shift MRI in distinguishing clear cell renal cell carcinoma from non-clear cell renal cell carcinoma and minimal-fat angiomyolipoma. AJR Am J Roentgenol 2015;205:W79—86.
[54] Rosenkrantz AB, Hindman N, Fitzgerald EF, Niver BE, Melamed J, Babb JS. MRI features of renal oncocytoma and chromophobe renal cell carcinoma. AJR Am J Roentgenol 2010;195:W421—7.
[55] Somford DM, Hambrock T, Hulsbergen-van de Kaa CA, Futterer JJ, van Oort IM, van Basten JP, et al. Initial experience with identifying high-grade prostate cancer using diffusion-weighted MR imaging (DWI) in patients with a Gleason score </= 3 + 3 = 6 upon schematic TRUS-guided biopsy: a radical prostatectomy correlated series. Invest Radiol 2012;47:153—8.
[56] Oto A, Yang C, Kayhan A, Tretiakova M, Antic T, Schmid-Tannwald C, et al. Diffusion-weighted and dynamic contrast-enhanced MRI of prostate cancer: correlation of quantitative MR parameters with Gleason score and tumor angiogenesis. AJR Am J Roentgenol 2011;197:1382—90.
[57] Rosenkrantz AB, Niver BE, Fitzgerald EF, Babb JS, Chandarana H, Melamed J. Utility of the apparent diffusion coefficient for distinguishing clear cell renal cell carcinoma of low and high nuclear grade. AJR Am J Roentgenol 2010;195:344—51.
[58] Goyal A, Sharma R, Bhalla AS, Gamanagatti S, Seth A, Iyer VK, et al. Diffusion-weighted MRI in renal cell carcinoma: a surrogate marker for predicting nuclear grade and histological subtype. Acta Radiol 2012;53:349—58.
[59] Wang H, Cheng L, Zhang X, Wang D, Guo A, Gao Y, et al. Renal cell carcinoma: diffusion-weighted MR imaging for subtype differentiation at 3.0 T. Radiology 2010;257:135—43.
[60] Cornelis F, Grenier N. Multiparametric magnetic resonance imaging of solid renal tumors: a practical algorithm. Semin Ultrasound CT MR 2017;38:47—58.
[61] Pedrosa I, Alsop DC, Rofsky NM. Magnetic resonance imaging as a biomarker in renal cell carcinoma. Cancer 2009;115(Suppl):2334—45.
[62] Pedrosa I, Chou MT, Ngo L, H Baroni R, Genega EM, Galaburda L, et al. MR classification of renal masses with pathologic correlation. Eur Radiol 2008;18:365—75.
[63] Roy Sr C, El Ghali S, Buy X, Lindner V, Lang H, Saussine C, et al. Significance of the pseudocapsule on MRI of renal neoplasms and its potential application for local staging: a retrospective study. AJR Am J Roentgenol 2005;184:113—20.
[64] Cornelis F, Lasserre AS, Tourdias T, Deminiere C, Ferriere JM, Bras YL, et al. Combined late gadolinium-enhanced and double-echo chemical-shift MRI help to differentiate renal oncocytomas with high central t2 signal intensity from renal cell carcinomas. AJR Am J Roentgenol 2013;200:830—8.
[65] Oliva MR, Glickman JN, Zou KH, Teo SY, Mortele KJ, Rocha MS, et al. Renal cell carcinoma: t1 and t2 signal intensity characteristics of papillary and clear cell types correlated with pathology. AJR Am J Roentgenol 2009;192:1524—30.
[66] Roy C, Sauer B, Lindner V, Lang H, Saussine C, Jacqmin D. MR Imaging of papillary renal neoplasms: potential application for characterization of small renal masses. Eur Radiol 2007;17:193—200.
[67] Kim JK, Kim SH, Jang YJ, Ahn H, Kim C-S, Park H, et al. Renal angiomyolipoma with minimal fat: differentiation from other neoplasms at double-echo chemical shift FLASH MR imaging. Radiology 2006;239:174—80.
[68] Rosenkrantz AB, Hindman N, Fitzgerald EF, Niver BE, Melamed J, Babb JS. MRI features of renal oncocytoma and chromophobe renal cell carcinoma. AJR Am J Roentgenol 2010;195:W421—7.
[69] Vargas HA, Delaney HG, Delappe EM, Wang Y, Zheng J, Moskowitz CS, et al. Multiphasic contrast-enhanced MRI: single-slice versus volumetric quantification of tumor enhancement for the assessment of renal clear-cell carcinoma Fuhrman grade. J Magn Reson Imaging 2013;37:1160—7.
[70] Sandrasegaran K, Sundaram CP, Ramaswamy R, Akisik FM, Rydberg MP, Lin C, et al. Usefulness of diffusion-weighted imaging in the evaluation of renal masses. AJR Am J Roentgenol 2010;194:438—45.
[71] Rosenkrantz AB, Oei M, Babb JS, Niver BE, Taouli B. Diffusion-weighted imaging of the abdomen at 3.0 Tesla: image quality and apparent diffusion coefficient reproducibility compared with 1.5 Tesla. J Magn Reson Imaging 2014;33:128—35.
[72] Bird VG, Kanagarajah P, Morillo G, Caruso DJ, Ayyathurai R, Leveillee R, et al. Differentiation of oncocytoma and renal cell carcinoma in small renal masses (<4 cm): the role of 4-phase computerized tomography. World J Urol 2011;29:787—92.
[73] Vargas HA, Chaim J, Lefkowitz RA, Lakhman Y, Zheng J, Moskowitz CS, et al. Renal cortical tumors: use of multiphasic contrast-enhanced MR imaging to differentiate benign and malignant histologic subtypes. Radiology 2012;264:779—88.
[74] Galmiche C, Bernhard JC, Yacoub M, Ravaud A, Grenier N, Cornelis F. Is Multiparametric MRI useful for differentiating oncocytomas from chromophobe renal cell carcinomas? AJR Am J Roentgenol 2017;208:343—50.
[75] Schieda N, McInnes MD, Cao L. Diagnostic accuracy of segmental enhancement inversion for diagnosis of renal oncocytoma at biphasic contrast enhanced CT: systematic review. Eur Radiol 2014;24:1421—9.
[76] Delahunt B, Sika-Paotonu D, Bethwaite PB, McCredie MR, Martignoni G, Eble JN, et al. Fuhrman grading is not appropriate for chromophobe renal cell carcinoma. Am J Surg Pathol 2007;31:957—60.
[77] Volpe A, Mattar K, Finelli A. Contemporary results of percutaneous biopsy of 100 small renal masses: a single center experience. J Urol 2008;180:2333.

Please cite this article in press as: Schieda N, et al. Characterization of small (<4 cm) solid renal masses by computed tomography and magnetic resonance imaging: Current evidence and further development. Diagnostic and Interventional Imaging (2018), https://doi.org/10.1016/j.diii.2018.03.004

[78] Choi SY, Sung DJ, Yang KS, Kim KA, Yeom SK, Sim KC, et al. Small (<4 cm) clear cell renal cell carcinoma: correlation between CT findings and histologic grade. Abdom Radiol 2016;41:1160—9.

[79] Romis L, Cindolo L, Patard JJ, Messina G, Altieri V, Salomon L, et al. Frequency, clinical presentation and evolution of renal oncocytomas: multicentric experience from a European database. Eur Urol 2004;45:53—7.

Please cite this article in press as: Schieda N, et al. Characterization of small (<4 cm) solid renal masses by computed tomography and magnetic resonance imaging: Current evidence and further development. Diagnostic and Interventional Imaging (2018), https://doi.org/10.1016/j.diii.2018.03.004